Estimate of the Energy of Upgoing Muons with Multiple Coulomb Scattering

D. Bakari [*], Y. Becherini, M. Spurio

(For the MACRO Collaboration)

Dipartimento di Fisica dell'Universitá di Bologna and INFN

Viale Berti Pichat 6/2 - 40137 Bologna (Italy)

[*] also LPTP, University Mohamed I, B.P. 524 Oujda (Morocco)

February 7, 2008

Abstract

[1] Upward throughgoing muons in underground detectors are induced by atmospheric ν_μ with energies in the $1 - 10^4$ GeV range. The oscillations of atmospheric muon neutrinos should affect mainly those with energy smaller than $E_\nu \sim 50$ GeV, or $E_\mu \leq 10$ GeV. We analyzed the MACRO[2] upward throughgoing muons data set, using the Multiple Coulomb Scattering to estimate the energy E_μ of muons crossing the detector. We analyzed the event distribution for six event subsamples with different values of $< \ell_\nu/E_\nu >$. The event distribution is in agreement with the hypothesis of neutrino oscillations with Δm^2 few times 10^{-3} eV^2 and maximum mixing.

1   Introduction

Neutrino oscillations, in a two neutrino mixing scenario, are the most likely solution for the *atmospheric neutrino problem* [1]. Underground experiments unfold the mass difference $\Delta m^2 = m^2_{\nu_3} - m^2_{\nu_2}$ and the mixing angle θ from the measurement of the survival probability

$$P(\nu_\mu \rightarrow \nu_\mu) = 1 - sin^2 2\theta \, sin^2(1.27\Delta m^2 \ell_\nu/E_\nu)$$

The survival probability is usually plotted versus the *measurable* quantities ℓ_ν and/or E_ν. ℓ_ν is the neutrino path length, estimated from the measurement of

---

[1]Invited contribution to the NATO Advanced Research Workshop: *Cosmic Radiation: From Astronomy To Particle Physics*, 21-23 March 2001, Oujda (Morocco)

[2]For a complete list of the MACRO Collaboration see the F. Ronga contribution to these Proceedings

the zenith angle Θ of the daughter lepton. The neutrino energy E_ν is estimated from the calorimetric measurement of the energy of all final state particles.

At present, E_ν is measured with some accuracy for low energy events (fully and partially contained SK [2] and Soudan2 [3] events); however in this case ℓ_ν is poorly reconstructed. The *vice versa* happens, when in the final state only the high-energy muon is measured (high energy neutrinos interacting in the rock around the detector, and inducing up-throughgoing muons in MACRO [7], SK [5] and Baksan[6]). The goal of next generation of atmospheric ν experiments should be the measurement of both ℓ_ν and E_ν, with enough precision to observe the first minimum of $P(\nu_\mu \to \nu_\mu)$.

In the case of the MACRO experiment, the measured oscillations parameters (best value: $\Delta m^2 = 2.5 \times 10^{-3} \ eV^2$ and $sin^2 2\theta = 1$) are deduced: from the deficit and the distortion of the zenith angle distribution of up throughgoing μ (*i.e.* $P(\nu_\mu \to \nu_\mu)$ *vs.* $cos\Theta$) [4, 7]; from the measured deficit of lower energy partially contained events[8].

In this paper we present the following approach: we identified topologies of upgoing muons induced from neutrinos with different energies and path length ℓ_ν, and we discuss the results in terms of ν_μ oscillations. The energy E_μ of detected muons is estimated through the multiple Coulomb scattering; E_μ is correlated with the energy E_ν of the parent neutrino. The survival probability shows a dependence with the $< \ell_\nu/E_\nu >$ parameter, unexpected without neutrino oscillations, while it is in good agreement with the quoted oscillation parameters.

2   Up throughgoing muon energy separation

Up throughgoing muons are induced both by (relatively) low energy atmospheric ν_μ, interacting near the detector, and higher energy neutrinos, interacting farther. Assuming the neutrino oscillations mechanism, with $\Delta m^2 = 2.5 \times 10^{-3} \ eV^2$ and $sin^2 2\theta = 1$, a reduced flux of muons with $E_\mu \le 10 \ GeV$ is expected, as shown by the shadowed histogram of Fig. 1a.

Multiple Coulomb Scattering. Muons traversing the detector are deflected by many small-angle scatters, the bulk of which are Coulomb scatterings from the nuclei and from the atomic electrons (Multiple Coulomb Scattering, MCS). As an effect, muons are slightly deviated from a straight-line direction by an angular deflection (projected in a plane) ϕ_{plane} [9]. Quantitatively, the averaged angular deflection ϕ_{plane}^{rms} and the spatial deflection y^{rms} in one projective plane are approximated with:

$$\phi_{plane}^{rms} = \frac{13.6 \ MeV}{E_\mu} \sqrt{\frac{x}{X_0}} [1 + 0.04 ln(\frac{x}{X_0})] \tag{1}$$

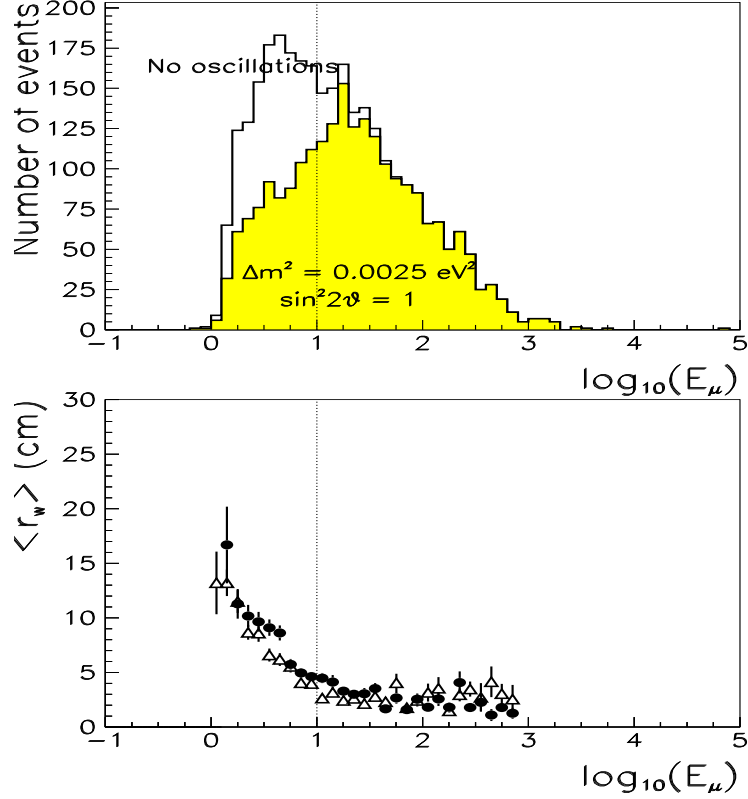$$y^{rms} = 1/\sqrt{3} \cdot x \cdot \phi_{plane}^{rms} \tag{2}$$

Figure 1: a) upper: energy spectrum of simulated neutrino-induced up throughgoing μ in MACRO. Full histogram for no oscillations; shadowed histogram, for $(\nu_\mu \to \nu_x)$ oscillations, with $\Delta m^2 = 2.5 \times 10^{-3}\ eV^2$ and $sin^2 2\theta = 1$. b) lower: profile of the averaged value of the parameter r_w $vs.$ muon energy. The full (open) points refers to events generated with the $full$ ($table$) MC simulation, see text.

In the case of MACRO, whose radiation length is $X_0 = 22.6\ gr/cm^2$ and total thickness $x = 400\ gr/cm^2$, the average angular deflection is $\phi_{plane}^{rms} \simeq 0.052\ (rad)/E_\mu\ (GeV)$. This corresponds to a projected spatial deflection in the wires view of the limited streamer tubes (whose cell size is 3 cm) of $y^{rms} \simeq 7(cm)/E_\mu(GeV)$.

Experimental technique. The technique we used to distinguish muons of low and high energy is illustrated in Fig. 2. All up throughgoing μ, crossing the whole apparatus, were analyzed. The streamer tube hits in the lowest planes (N=1:8) were used for a refit, and the straight-line fit parameters were used to define the *lower track*. In a similar way, the highest planes (N=6:14) were used to define the *upper track*. The upper and lower tracks are used to evaluate r_w, the spatial difference in the $z = 0$ plane between the two tracks, and $\Delta\Phi$, the angular difference between the slopes. The value of the parameter r_w $(\Delta\Phi)$ depends on the muon energy E_μ. In Fig. 1b the profile (*i.e.* the average value of r_w evaluated in each bin of E_μ from our MC events) is shown. From the figure, the spatial difference between the lower and upper track exceed the intrinsic resolution of streamer tube cells when $E_\mu < 10\ GeV$. The behavior of the $\Delta\Phi$ parameter is analogous.

Event classification. A selection cut, based on r_w and $\Delta\Phi$, was defined. Each up throughgoing muon is classified as: $L=$ *Low energy* if $r_w > 3\ cm$ and $\Delta\Phi >$
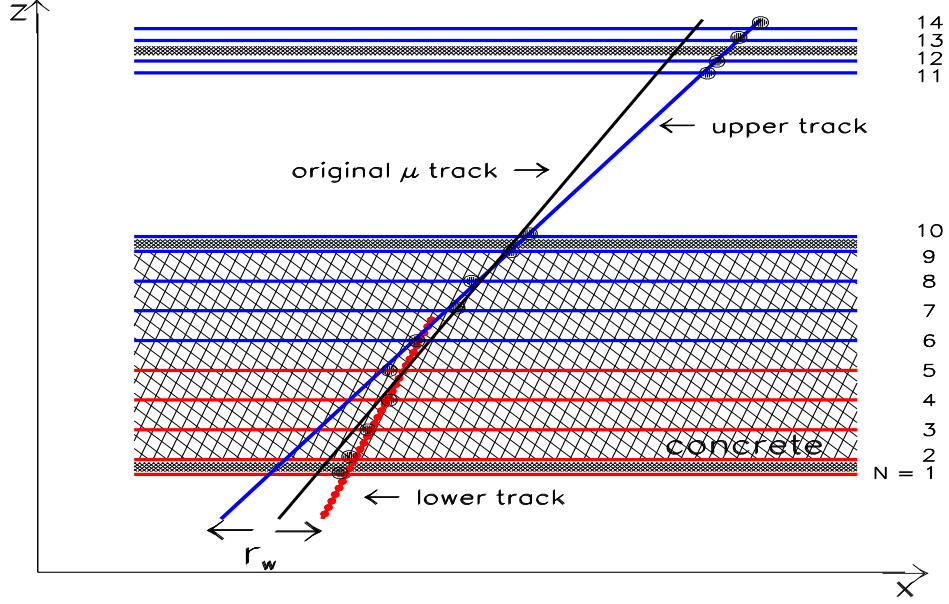
Figure 2: Sketch of the refit procedure to obtain a *lower* and an *upper* track, and the definition of the parameter r_w.

0.3^o; *H= High energy* if $r_w \leq 3\ cm$ and $\Delta\Phi \leq 0.3^o$. The remaining events with ambiguous deviation, were classified as *M=Medium energy*. Each sub sample has a different average energy for the parent neutrino. If ν_μ disappearance is at work, the reduction should affect mainly the L sample, and we expect in the data a reduced $\frac{L}{H}$ ratio, with respect to the MC prediction without oscillations.

Checks on Monte Carlo predictions. A crucial point is the MC reliability, to avoid any systematic bias which can invalidates the results. For a detailed check of the detector simulation, we compared two large samples of measured with simulated downward going atmospheric muons. Down throughgoing atmospheric muons have an average residual energy of $\sim 300\ GeV$ when reaching the underground laboratory, and 90% of them have $E_\mu > 10\ GeV$. Our cut classified 63% (25%) of these events as *H*igh (*L*ow) energy. The small fraction of atmospheric muons ($\sim 0.3\%$), reaching MACRO with $E_\mu \leq 1 - 5\ GeV$, stops inside the detector: 88% (7%) of them have been classified as *Low* (*High*) energy.

The energy distribution of these two atmospheric samples overlaps the spectrum of neutrino-induced upgoing μ: the down-stop events in the lower, and the down- throughgoing in the high-energy tail. Using atmospheric muon samples, we adjusted the streamer tubes geometry in the MC database. After the MC correction, the measured and expected distribution of r_w and $\Delta\Phi$ variables match together, both for the down-stop and down-throughgoing atmospheric muons.

3   Results

Real data. We used the same up throughgoing muon sample described in [1]a. The details of the events identification, cuts and selection efficiency were published [4, 7]. In our analysis, only the 316 events crossing the whole apparatus where used, to enhance the MCS effect on the muon track. The r_w and $\Delta\Phi$ parameters are evaluated from the reconstructed *lower* and *upper* tracks, and 101 events were classified by the cuts as *Low*, 51 as *Medium* and 164 as *High* energy.

Simulated data. The expected number of up throughgoing muons from ν_μ interactions was evaluated with two different methods. In the first method ("table" MC) [4, 7], the muon energy spectrum is obtained from a numerical convolution of the differential atmospheric neutrino spectrum, neutrino cross-sections and muon propagation in the rock. In the second ("full" MC), a full simulation is used: the ν_μ interact in a large volume of rock around the detector, and the muon is propagated through the rock up to the detector. The simulated data have the same format of the real ones, and thus followed the same analyses steps. We applied the cut on r_w and $\Delta\Phi$ on the selected up throughgoing MC muons: for a live time period equivalent of that of the real data, we expect 431 (430) events from "table" ("full") MC: 177 (178) L, and 191 (193) H.

Uncertainties. The overall theoretical uncertainty on MC predictions is 17% [1,2]. This is a scale factor, which is almost constant when the number of events is plotted versus $cos\Theta$ or E_ν. The shape of the distributions (as the angular one presented in [4, 7]) has a reduced theoretical uncertainty: we assumed a (conservative) value of 5% in the considered range of ν energies. The systematic uncertainties depend from many factor: the number of upper/bottom planes used in the refit; the choice of a particular value of r_w and $\Delta\Phi$; the MC simulation statistics; the fluctuation in the streamer tube and scintillator efficiency along the running period; the detector acceptance uncertainty vs. the muon zenith angle. The evaluated overall systematic uncertainty is 7%.

Data and MC comparisons. We divided the events in three bins of E_μ (L, M, H). The L and H samples were sub-divided in two bins of neutrino path length variable ℓ_ν (the Medium energy sample have too few events). The number of detected and expected events $vs. < log_{10}(\ell_\nu/E_\nu) >$ (MC evaluated) is presented in Table 1 and Fig. 3. It is also included an additional point, corresponding to the partially contained IU events [8]. These events are induced by neutrinos with an average energy $E_\nu \sim 4\ GeV$, interacting inside the detector. This sample is contaminated by a 13% contribution of ν_e and NC interactions.

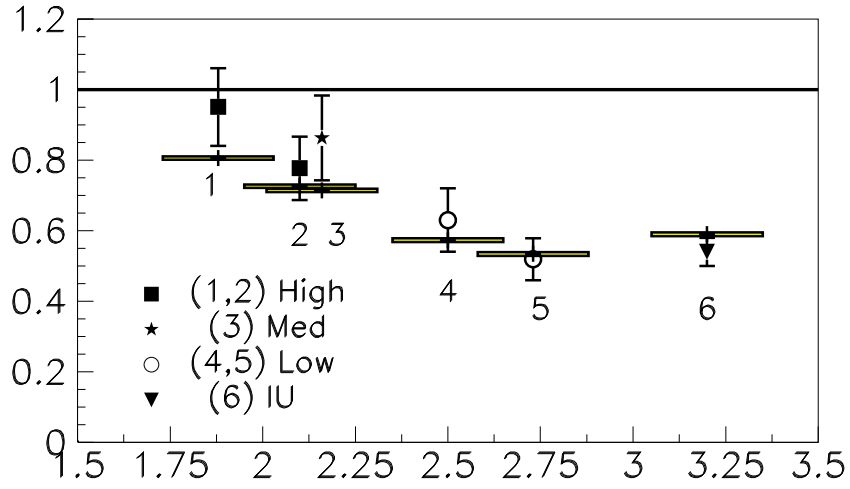The ratio R between the detected to the expected number of events for

Figure 3: Ratio R of the measured to the expected number of events vs. $< log_{10}(\ell_\nu/E_\nu) >$. The H and L samples are subdivided in two intervals of ℓ_ν. The black triangle is the point corresponding to the partially contained upgoing events is included [4]. The horizontal full line represents the expectation assuming no oscillations. The segment below each data point is the expectation assuming $\nu_\mu \rightarrow \nu_x$, with oscillation parameters quoted in Fig. 1a).
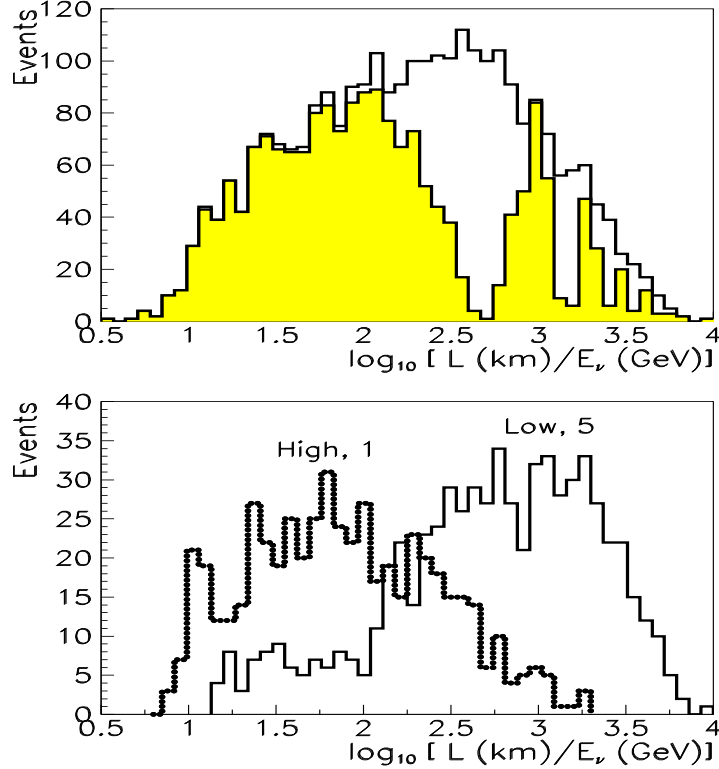

Figure 4: a) Full histogram: simulated distribution of reconstructed up through-going muons in MACRO vs. $log_{10}(\ell_\nu/E_\nu)$. The shadowed region represents the expected distribution in case of neutrino oscillations (with the parameters of Fig. 1a). b) The full histogram corresponds to the distribution of simulated neutrino-induced muons, classified of high-energy from the Multiple Coulomb Scattering analysis, and with large zenith angle. The dashed histogram is for low-energy muons, with small zenith angle. The average value of these two distributions, are plotted in Fig. 3 (points 1 and 5).

	zenith	$< log_{10}(\ell_\nu/E_\nu) >$	N_{data}	N_{MC}	N_{MC}^{osci}
H (1)	$|\cos\Theta| < 0.8$	1.89 ± 0.55	76	80	64
H (2)	$0.8 < |\cos\Theta| < 1.0$	2.11 ± 0.55	88	113	82
M (3)	$0 < |\cos\Theta| < 1.0$	2.16 ± 0.66	51	59	42
L (4)	$|\cos\Theta| < 0.8$	2.50 ± 0.56	47	74	43
L (5)	$0.8 < |\cos\Theta| < 1.0$	2.72 ± 0.60	54	104	56
IU (6)	$0 < |\cos\Theta| < 1.0$	~ 3.2	154	285	168

Table 1: Number of detected and expected events (N_{data}= detected, N_{MC}= expected and N_{MC}^{osci}=expected with oscillations). In column 3, there is the average value $\pm$ the HWHM of the $log_{10}(\ell_\nu/E_\nu)$ distribution.

each sub sample is shown in Fig. 3. The value of R expected with the used flux and neutrino cross sections, is 1 (no oscillations). This value has an overall scale factor uncertainty of 17%, which is almost constant all over the (ℓ_ν/E_ν) interval. In our data, R decreases when $< log_{10}(\ell_\nu/E_\nu) >$ increases. This behavior is consistent with the neutrino disappearance probability, when folded with our distribution of events. In Fig. 3 the segment below each data point is obtained from Monte Carlo simulated events, assuming oscillation parameters $\Delta m^2 = 2.5 \times 10^{-3}\ eV^2$, $sin^2 2\theta = 1$. The effect of neutrino oscillations in the distribution of (ℓ_ν/E_ν) is shown in Fig. 4a as a shadowed histogram. The effect of our cuts on the simulated events is shown in Fig. 4b for two subsamples (the one with the lowest/highest average value of (ℓ_ν/E_ν)).

We evaluated the χ^2 for the shape of the ratio R vs. $< log_{10}(\ell_\nu/E_\nu) >$ for the two different test hypotheses: T0= no and T1= neutrino oscillations with the above quoted parameters. For hypothesis T0, we expect a (almost) constant value. Normalizing the number of expected with the number of detected events (316/430), we get a $\chi^2/dof = 14.8/5$ (probability of less than 2%). For hypothesis T1 we expect a value of R which decreases as a "ladder" from 1 to 1/2, when $(\ell_\nu/E_\nu) > 1000\ Km/GeV$. In this case, we get $\chi^2/dof = 4.7/5$ (probability=45%)

Hypotheses T0 and T1 can be tested also using the ratio of ratios $(\frac{L}{H})_{data}/(\frac{L}{H})_{MC}$. With the double ratio, most of the theoretical and systematic uncertainties cancel. For T1, we expect a larger reduction of events with Low energy with respect to the ones with $High$ energy. From our data, $(\frac{L}{H})_{data} = 0.62 \pm 0.08$. For T0, $(\frac{L}{H})_{MC}^{T0} = 0.92 \pm 0.08$ (c.l. of 0.5%). For T1 $(\frac{L}{H})_{MC}^{T1} = 0.68 \pm 0.06$ (c.l. 90%).

4 Conclusions

We discussed the possibility to study the present high-energy atmospheric neutrinos data in terms of different bins of $< log_{10}(\ell_\nu/E_\nu) >$, using the Multiple Coulomb Scattering on muons. The MACRO events were analyzed: the result is consistent with the hypothesis of neutrino disappearance with $\Delta m^2 = 2.5 \times 10^{-3}\ eV^2$ and $sin^2 2\theta = 1$. This strengthens the hypothesis of neutrino oscillations to explain the data, against alternative more exotic models. A global analysis of all MACRO neutrino-induced data sets (which includes the results of this work) is in progress.

References

[1] See also F. Ronga, D. Michael and E. Scapparone talks on this workshop

[2] Y. Fukuda et al. (Super-Kamiokande Coll.) Phys.Rev.Lett. 81 (1998) 1562

[3] W.A. Mann (Soudan 2 Collaboration), Nucl. Phys. Proc. Suppl. 91 (2000)134.

[4] S.Ahlen et al. (MACRO Collaboration), Phys.Lett. B357 (1995)481

[5] Y. Fukuda et al. (Super-Kamiokande Coll.) Phys.Rev.Lett. 82 (1999) 2644

[6] See S. Mikheyev at SNO2000 http://nu2000.sno.laurentian.ca/

[7] M.Ambrosio et al. (MACRO Collaboration), Phys. Lett. B434 (1998)451.

[8] M.Ambrosio et al. (MACRO Collaboration), Phys.Lett. B478 (2000)5

[9] Review of Particle Physics (Particle Data Group) Eur.Phys.J.C3(1998)